International Journal of Innovative Computing, Information and Control
Volume **20**, Number **1**, February **2024**

ICIC International ©2024 ISSN 1349-4198
pp. **15–30**

RESEARCH AND APPLICATION OF INTELLIGENT DETECTION TECHNOLOGY FOR BRIDGE GIRDER BOTTOM APPEARANCE DEFECTS BY SUSPENDED BRIDGE INSPECTION VEHICLE

Jun Xu[1,2], Qingrong Jia[3], Tingqi Qiu[4,*], Yuanqing Xu[5], Minglong Wu[4] and Bing Yang[4]

[1]College of Civil Engineering
Tongji University
No. 1239, Siping Road, Shanghai 200092, P. R. China
x861@163.com

[2]CCCC Highway Consultants Co., Ltd.
No. 33, Qianchaomian Hutong, Dongcheng District, Beijing 100010, P. R. China

[3]Guangdong Bay Area Transportation Construction Investment Co., Ltd.
Room 301, No. 1, Qilin Second Street, Huangge Town, Nansha District
Guangzhou 510000, P. R. China
xuqingrong202302@126.com

[4]Chengdu Xinzhu Road & Bridge Machinery Co., Ltd.
Sichuan Xinjin Industrial Park, Chengdu 611400, P. R. China
xinzhujiaoke2021@126.com; yangbing19830816@163.com
*Corresponding author: xinzhujiaoke2021@163.com

[5]CCCC Highway Bridges National Engineering Research Centre Co., Ltd.
302, 3rd Floor, No. 85, Deshengmenwai Street, Xicheng District, Beijing 100032, P. R. China
xuyuanqing470@163.com

Received March 2023; revised July 2023

Abstract. *With the increase of service time, different degrees of damage appear on the surface of the bridge. It increases the safety hazard of the bridge. Regular inspection of bridge appearance can effectively prevent safety accidents. However, the existing bridge defect detection technology has low efficiency and precision in the detection process. Meanwhile, they are greatly affected by environmental factors, and do not have wide applicability. Accordingly, the suspended bridge inspection vehicle is designed to carry out intelligent detection of bridge appearance defects. Aiming at the low accuracy in the image recognition process in the inspection vehicle, the attention mechanism is used to improve the image recognition system. At the same time, the findContours function is used to track the contour image and calculate the image defects. The results show that the abnormal detection accuracy rate of the STPM+AM model in the suspended bridge inspection vehicle is 98.8%, which is 1.7% higher than that of the STPM model. The calculated defect crack width error is about 0.03 mm. The crack length error is around 1.5 mm. Therefore, the suspended bridge inspection vehicle proposed in the study has high efficiency and accuracy in the detection of bridge appearance defects, which can effectively meet the actual needs of bridge maintenance.*

Keywords: Bridge inspection vehicle, Appearance defect, Intelligent inspection, STPM, Attention mechanism

DOI: 10.24507/ijicic.20.01.15

1. **Introduction.** Under the background of rapid development in transportation industry, bridges, as an important part of all kinds of transportation infrastructure, effectively solve the connection problem of highways and railways under the influence of topography and geology [1]. Under the action of various external forces, the completed bridge structure will suffer from various damages, including impact, parts falling off and cracks. Bridge cracks are the most common among them. When conducting defect detection, traditional manual detection methods are inefficient, low accuracy, high economic and time costs. The subjective impact has a significant influence on manual detection, which cannot meet the detection needs of modern large-scale bridges [2]. With the improvement and development of process technology, the bridge detection method has developed from the initial manual observation, judgment and positioning to the identification and judgment of bridge defects relying on intelligent technology [3]. Jeong et al. combined the UAV detection image with grayscale enhancement technology to better identify and measure defects in bridges. The results show that drone detection image enhancement technology can demonstrate the adjustment and improvement of defects, thereby more reliably identifying and measuring defects in bridges [4]. Ye et al. proposed a bridge weld defect detection method based on machine vision combined with weak magnetic technology. The results indicate that the method of combining machine vision and magnetism can accurately identify the location of defects. At the same time, surface and internal defects of bridges can be classified and the equivalent size of defects can be estimated [5]. Scholars have innovated the inspection methods for bridge defects from multiple perspectives. Commonly used intelligent detection methods include optical fiber sensing detection, ultrasonic detection, radar detection and infrared detection. However, these detection techniques are greatly affected by environmental factors. The operation is relatively complicated, and the cost is high [6]. Attention Mechanism (AM), as a deep learning method, has unique advantages in image feature extraction. Therefore, in response to this problem, a suspended bridge inspection vehicle is proposed to detect bridge appearance defects. The attention mechanism is used to build an image recognition model. Through this identity authentication protocol, the intelligent detection technology of bridge appearance defects is improved to meet the needs of bridge appearance defect detection. The experiment found that the AUC value of the bridge defect inspection model proposed in the study was 0.968, with an accuracy of 98.8%. The error in crack length obtained from the study is around 1.5 mm. The crack error data detected by the algorithm is relatively small and distributed within a reasonable interval class, indicating that the crack calculation method proposed in the study is effective.

The contributions of this study are as follows. Firstly, in order to improve the recognition accuracy of image defects during the inspection of bridge appearance defects, attention mechanism was introduced to improve the image recognition method, achieving accurate recognition of bridge defects. Then, the findContours function was used to quantify bridge defects and achieve specific calculations for bridge defects. The main innovation of the research is twofold. The first point is to use attention mechanisms to achieve intelligent and efficient recognition of bridge defect images. The second point is to use the findContours function in the OpenCV library for specific tracking calculations of bridge defects. The existing detection and recognition technologies for bridge defects mainly focus on obtaining bridge defect images. There is relatively little quantitative research on specific bridge defects. Therefore, compared to existing research, this study not only extracts bridge defect images in more detail, but also calculates the specific trend of defect changes to help relevant personnel better maintain bridge performance.

The study consists of five parts. The first one is introduction. The second part provides a research review on bridge defect inspection methods and attention. The third part

constructs a bridge defect detection technology based on a suspended bridge inspection vehicle, including preprocessing of bridge defect images, image recognition methods based on attention mechanism, and calculation methods for bridge defects. The fourth part conducts experimental verification on the performance of the bridge defect detection method proposed in the study. The fifth part summarizes the entire article and proposes future research directions.

2. **Related Work.** Affected by factors such as the natural environment and early construction, there are various degrees of damage and defects. Therefore, it is necessary to carry out regular maintenance. Ayele et al. used Unmanned Aerial Vehicles (UAV) to inspect and maintain the bridge. Deep learning was introduced into the bridge damage detection and analysis method. In the experiment, this method can effectively reduce the time and economic cost of bridge inspection, improving the detection accuracy [7]. Ikeda et al. designed a bridge detection method focusing on visual inspection. A manipulator is installed on the top of the UAV, which can control in three directions. In the experiment, the camera control method proposed in the study reduces the error. It can effectively obtain images of narrow spaces such as bearings in bridges [8]. Minkina used infrared cameras to detect the faults of high-voltage lines in substations. The early fault warning information was obtained. The stability and safety of current transmission were improved [9]. Combining robot and computer vision technology, Li et al. proposed a bridge crack detection and recognition method based on convolutional neural network, which immediately converted the extracted damage map into a global bridge damage map. The image capture and geotagging were used to get georeferenced data. The possibility of obtaining damage maps in time was demonstrated [10]. Won et al. used the depth matching splicing method to splice the bridge images. The panoramic image of the bridge were obtained to locate and quantify the loss of the bridge. Experiments have shown that the method successfully generates panoramic images with a minimum incidence of ghosting and drifting [11]. Based on the statistical data of the bridge monitoring system, Zhao et al. designed a crack assessment and early warning method for prestressed concrete beam bridges. Gauss mixture model is used to cluster the strain characteristics caused by vehicles. The bridge cracking warning is conducted according to the reliability of heavy vehicle clustering data. The result proves that the test accuracy of this method exceeds 99%. It can be effectively applied to bridge maintenance work [12].

Attention mechanism is the key research object in the field of deep learning, which is widely used in the field of intelligent artificial. Yuan and Dai built a model to predict video frames, which combined LMST with attention mechanism to predict video frames in this way. In the experiment, the accuracy of video frame prediction has been significantly improved, and the images obtained are clearer and more realistic [13]. Cheng et al. used an improved attention mechanism to build a pipeline burst prediction model in analyzing the location of pipeline burst in the water supply network. The results prove that the analysis model based on the improved attention mechanism has better robustness and higher accuracy. This method provides an effective method for pipeline burst identification and inspection [14]. Huang et al. proposed an attention mechanism-based remote sensing image fusion network. A dual-channel feature extraction layer is used to extract the spatial features of PAN and the spectral features of MS, respectively. Experiments have proved that this algorithm is significantly better than traditional remote sensing image feature extraction methods [15]. Aiming at the problem that the tracking algorithm is prone to data loss under the condition of target deformation and external interference, Shao and Ge proposed a target tracking algorithm combined with residual connection and channel attention mechanism to enhance the model's ability to identify similar targets. The results

show that this algorithm has higher accuracy and efficiency [16]. Liu et al. proposed a generation model based on the attention mechanism for the significant defects of the generation model VAE and GAN in the image restoration process. In the experiment, the network model based on the attention mechanism has higher stability, effectively improving the resolution of generated images and the number of running frames [17]. Li et al. proposed a visual tracking algorithm that combines attention mechanism and convolutional neural network to effectively work out the kinks of complex environment affecting tracking performance. Experimental results prove that the tracking performance and success rate of this algorithm have been effectively improved [18].

To sum up, the detection of bridge defects and other infrastructure defects has been integrated into computer network technology. However, there is relatively insufficient research on the specific identification and calculation of defects. The AM has a significant advantage in image feature recognition. Therefore, aiming at this problem, the suspended bridge inspection vehicle is used as a carrier to build an image recognition system based on the AM. The AM is used in image feature extraction. It is hoped to improve the inspection effect of the bridge inspection vehicle on the appearance defects of the bridge girder bottom.

3. Bridge Defect Detection Technology Based on Suspended Bridge Inspection Vehicle.

3.1. Image preprocessing of bridge girder bottom appearance defects.

The traditional bridge detection mainly relies on human visual observation to determine the defect degree and location of the bridge. The bridge inspection vehicle is the carrier for the bridge maintenance staff to work during the maintenance process, which is mainly used for bridge maintenance and repair operations. The suspended bridge inspection vehicle is mainly composed of a lifting pole, a walkway above, walking parts and a detection and analysis system. When acquiring image information, a CMOS industrial camera is used as an image information acquisition device. The appearance defect of the bridge is an inevitable problem in the process of using the bridge. When using a detection vehicle to identify bridge appearance defects, the first step is to preprocess the obtained bridge appearance image. Generally speaking, a bridge defect image is divided into three color channels, namely, red, green and blue. The RGB value is divided into [0-255] interval values [19]. The horizontal and vertical coordinates of any point in the image are defined as (i, j). The gray value of the coordinate position is $Gray(i, j)$. The values of the three color channels are expressed as $R(i, j)$, $G(i, j)$ and $B(i, j)$, respectively. The value of the image channel is weighed to obtain the average value. The gray value obtained is shown in Formula (1).

$$Gray(i, j) = \frac{R(i, j) + G(i, j) + B(i, j)}{3} \tag{1}$$

Due to the influence of environment, lighting and other factors, the image needs to be enhanced to make the contrast between the image details more obvious. The histogram equalization is adopted to enhance the image. Through the histogram equalization process, the original image is converted into a histogram with relatively uniform gray level distribution. This enhances the difference between the image area and the background area, and improves the contrast between image information [20]. However, the image is often distorted in the process of formation, so it is necessary to expand the image linearly through the gray value. If the original image is $f(x, y)$, its gray scale range is $[a, b]$, the gray scale mapping image is $g(x, y)$, and its expanded range is $[c, d]$, the following Formula (2) is satisfied.

$$g(x,y) = \frac{d-c}{b-a} \times [f(x,y) - a] + c \tag{2}$$

Some pixels in the image are $[a, b]$ outside. To achieve the gray enhancement effect of the image, a piecewise linear function is used to perform gray enhancement transformation on the image, as shown in Formula (3).

$$g(x,y) = \begin{cases} c & 0 \le f(x,y) \le a \\ \dfrac{d-c}{b-a} \times [f(x,y) - a] + c & a \le f(x,y) \le b \\ b & b \le f(x,y) \le \max f \end{cases} \tag{3}$$

Several sub regions of the image gray level region are obtained in the piecewise linear transformation. Each sub region has the same size. Linear transformation enhances the target area and image contrast in the image. Finally, the image is denoised. The denoising method can adopt Mean Filtering Algorithm (Mean FA) and Median Filtering Algorithm (Median FA). Mean FA has the advantages of fast operation, simple algorithm and good filtering effect. However, it damages the image definition. Median FA makes up for the shortcomings of image damage [21]. The specific process is shown in Figure 1.

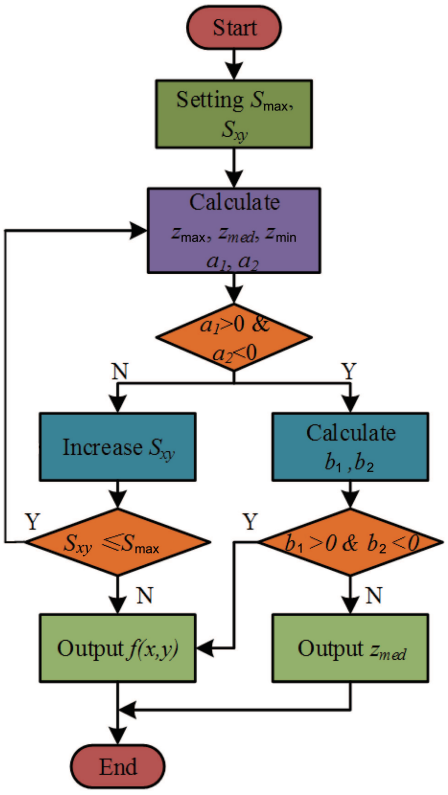

FIGURE 1. Basic flow of adaptive median filter algorithm

The image to be filtered is $f(x, y)$. The gray value is (x, y). The replacement value after gray value processing is $g(x, y)$. $S(x, y)$ represents a set of neighborhood pixels of the image to be filtered. $z_{\min}$, z_{med} and $z_{\max}$ represent the minimum value, median value and maximum value neighborhood pixel set in the $S(x, y)$ respectively. $S_{\max}$ represents the maximum template size. S_{xy} is the current template size. a_1 and a_2 are opposite numbers, representing the error between extreme value and median value. b_1 and b_2 are the same opposite numbers, representing the error between the gray value and the median value. In the above operation process, it is first determined whether z_{med} is impulse noise. If it

is impulse noise, $g(x, y) = f(x, y)$. If z_{med} belongs to impulse noise, the filter template size shall be processed. Adaptive median filtering can not only achieve the processing effect of mean filtering, but also can effectively avoid the image blurring. The image restoration effect is better [22]. Finally, the image is segmented. The Canny operator is used to simplify edge detection and calculate the maximum value of the unit function.

3.2. **Defect image recognition based on attention mechanism.** The bridge image obtained by the suspended bridge inspection vehicle needs to be pre-processed to detect anomalies in the images. Commonly used data anomaly detection models include CNN, DifferNet and STPM models. The STPM model is used in the central control system of the inspection vehicle to detect abnormal images. However, this detection model has low accuracy [23]. Therefore, an attention mechanism is introduced in the process of image recognition of inspection vehicles to extract features from image information. AM refers to scientifically assigning attention to important parts of the input sequence by simulating the attention model of the human brain, so as to achieve better learning information of the input sequence. This technology is widely used in natural language processing, statistical learning, image detection, speech recognition and other fields. The main idea is to determine the importance of each element based on a series of weight parameter ratios. Then, elements are combined based on their importance [24]. The calculation method of AM is shown in Formula (4).

$$Attention(Query, Source) = \sum_{a=1}^{L_u} p(r = a|Key_{1,N}, Query) \cdot Value_a \tag{4}$$

In Formula (4), *Query* indicates the given element in the input sequence. *Source* represents the input element. *Key* is the importance of each element. *Value* is the weight coefficient corresponding to each *Key*. This method can extract the key information in the image to be distinguished in a targeted manner, and ignore the relatively unimportant information. The workflow of the AM is shown in Figure 2.

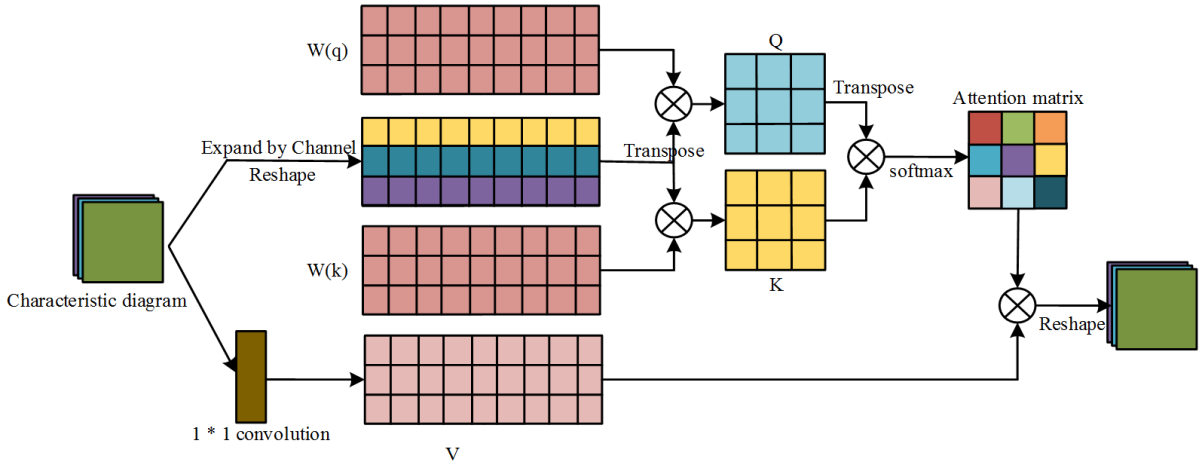

FIGURE 2. Flowchart of AM

From Figure 2, after inputting the acquired image information into the model, the AM is used to process the feature channels. When image processing, attention is focused on a specific part of the image, instead of processing all images. The key information in the image is extracted while ignoring irrelevant information. The corresponding image selection is completed [25]. Then the relationship between each channel is calculated. Finally, the corresponding weight matrix and feature map are output. Therefore, an STPM

anomaly detection model combined with AM is constructed. An AM is added in the feature extraction process, so that the residual network can effectively extract the main information in the image. The teacher network can better guide the student network to learn the extraction of image features. Firstly, the RGB image is input. Then, the teacher and the students respectively output the feature map F_s^l and F_t^l at the l layer. The feature vector at any feature map (i, j) position is $F_t^l(I_K)ij$ and $F_s^l(I_K)ij$. The loss at this point is shown in Formula (5).

$$I^l(I_K)ij = \frac{1}{2}\left\|F_t^l(I_K)ij - F_s^l(I_K)ij\right\|_{l_2}^2 \tag{5}$$

The total loss of the model is the weighted average of the loss values at different locations, as shown in Equation (6).

$$I^l(I_K) = \sum_{i=1}^{L} a_l I^l(I_K) \tag{6}$$

The abnormality at the position (i, j) is denoted by Ω, and $\Omega_{ij} \in [0, 1]$. The loss value at l layer any position (i, j) in the feature map is used to represent the abnormal size $\Omega^l(J)$. The bilinear interpolation method is used to obtain the abnormal map Ω with image information. The anomaly map with the same size in layer l is multiplied, as shown in Formula (7).

$$\Omega(J) = \prod_{l=1}^{L} Upsample\, \Omega^l(J) \tag{7}$$

Then, the maximum value Ω of the anomaly mapping is used as the judgment threshold for image anomalies. If the abnormal value of the image is greater than the predetermined threshold, it belongs to the defective image. If it is smaller than the predetermined threshold, it does not belong to the defective image.

3.3. **Measurement and calculation method of bridge bottom defects.** After the bridge defect image is obtained by attention mechanism, the length and width of the bridge defect are calculated. The findContours function in the OpenCV library is used to track the contour image. The minimum bounding rectangle is Rect. a_1 represents the length of the minimum circumscribed rectangle. a_2 represents the width of the minimum circumscribed rectangle. The ratio of a_1 to a_2 is X. The calculation method of X is shown in Formula (8).

$$X = \begin{cases} a_1/a_2, & a_1 > a_2 \\ a_2/a_1, & a_1 < a_2 \end{cases} \tag{8}$$

The ratio between the crack area and the perimeter in the connected domain is expressed by R. The calculation method of R is shown in Formula (9).

$$R = A/C \tag{9}$$

In Formula (9), A indicates the area of the crack in the connected domain, and C represents the perimeter of the crack in the connected domain. The circularity of cracks in the connected domain is represented by H. The calculation method is shown in Formula (10).

$$H = 4\pi \times \frac{A}{C^2} \tag{10}$$

After analyzing and comparing the above parameters, the conditional parameters for judging cracks are obtained as shown in Formula (11).

$$X > 1,\ R > 2,\ H < 0.5 \tag{11}$$

After determining the parameters of the crack determination conditions at the bottom of the bridge beam, the cracks can be automatically tracked and identified. After the bridge defect target is obtained, the obtained crack size is measured to evaluate the damage degree of the bridge defect. Firstly, the area A and arc H of the connected domain are calculated through the tracking and identification operation of the crack. Then the crack outline is skeletonized to calculate the number of white pixels in the crack's smallest circumscribed rectangle. The specific process is shown in Figure 3.

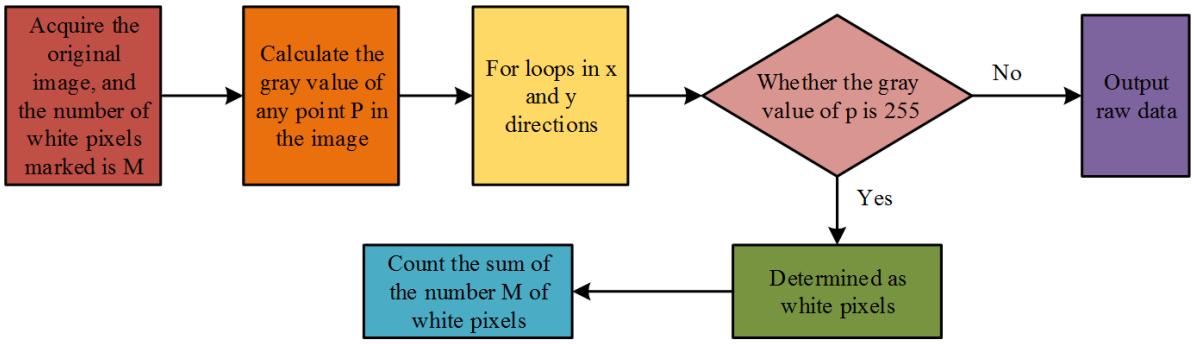

FIGURE 3. White pixel calculation process

After completing the statistics of the white pixels through the process in Figure 3, Formula (12) is used to calculate the average width of the crack.

$$W = A/L \tag{12}$$

In Formula (12), A refers to the area of the crack in the connected domain. L represents the length of the crack. From the known research, the value of R is 0.0125 mm/pixel. The calculation method of L is shown in Formula (13).

$$L = n \times R = n \times 0.0125 \tag{13}$$

In Formula (13), n represents the number of white pixels. Through the above-mentioned findContours function tracking method, the specific size of the defect contour at the bottom of the bridge girder can be calculated. The Visual Studio2013 is experimental platform. The image algorithm function in OpenCV is used to design the process. The intelligent inspection technology for appearance defects of bridge bottom is designed by using the inspection vehicle of suspension bridge. The image information is acquired by a CMOS camera [26]. Then the image data is preprocessed and classified. Finally, the crack size of the classified bridge appearance defect image is calculated. The specific process is displayed in Figure 4.

From the above process, a relatively complete set of operating algorithms for autonomous identification of bridge appearance defects and crack measurement has been formed in the system of the bridge inspection vehicle.

4. Performance Analysis of Bridge Defect Detection Technology Based on Suspended Bridge Inspection Vehicle.

4.1. Performance analysis of defect detection technology based on suspended bridge inspection vehicle. The Ubuntu 18.04 operating system is used in the experiment. Firstly, the performance of the data anomaly detection model in the bridge inspection vehicle is analyzed. 5000 image samples were divided into training and testing sets at a ratio of 3 : 7. The STPM model based on the AM proposed in the study is trained. The training results are shown in Figure 5.

FIGURE 4. Flowchart of intelligent detection of bridge defects

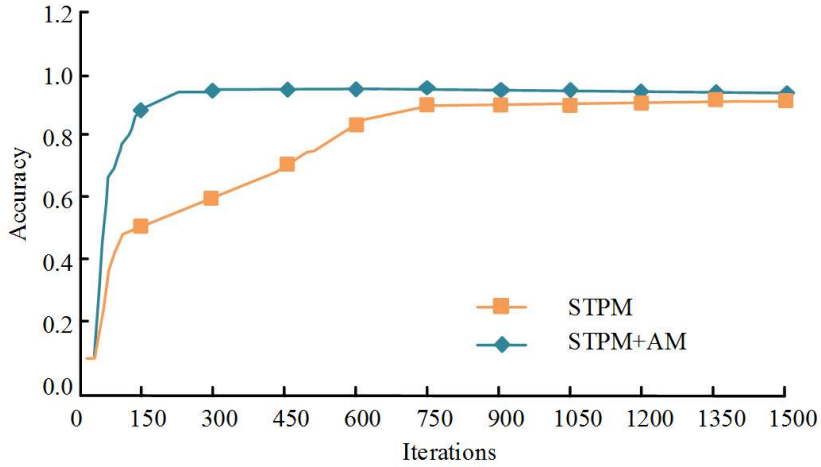

FIGURE 5. Comparison of training accuracy between two models

From Figure 5, as the number of samples increases, the accuracy of both models is improving. The more samples extracted, the model can extract richer image features, resulting in higher detection accuracy. When the training samples reach 1500, the accuracy of STPM model is 94.3%. The accuracy of STPM+AM model is 96.5%, which is 2.2% higher than STPM model. Therefore, the STPM model with attention mechanism has better accuracy.

The loss curves obtained from two abnormal image detection models are shown in Figure 6.

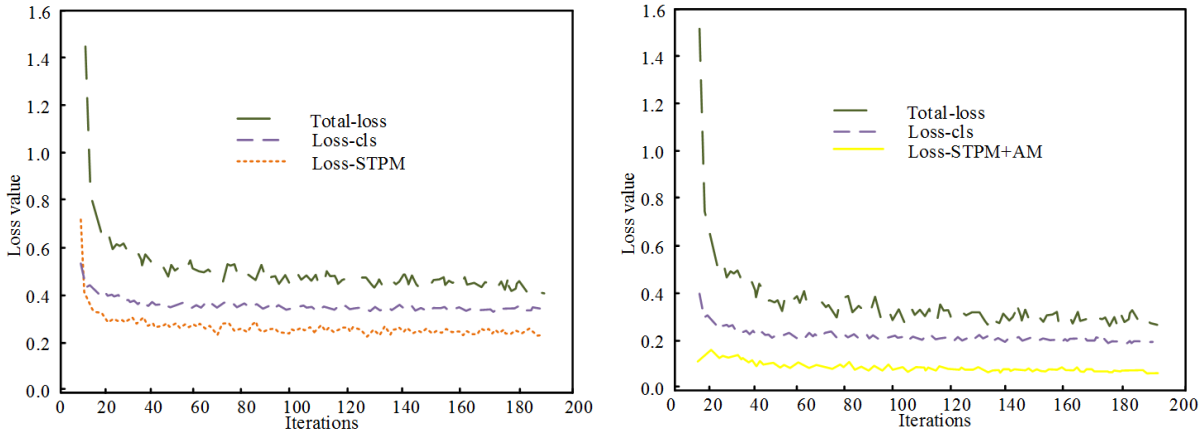

(a) Loss-STPM (b) Loss-STPM+AM

FIGURE 6. Loss function value of two models

In Figure 6, loss-cls is used to calculate the classification loss of the object detection algorithm. In the STPM anomaly detection model, the loss-cls starts to converge from the initial value of 0.56, and then tends to be stable after converging to 0.39. The loss-cls value of the STPM+AM model tends to be stable at 0.25, which is 0.14 lower than that of STPM. The loss of the STPM anomaly detection model gradually stabilizes after 20 iterations. When iterating 70 times, there is a significant fluctuation. The loss value of the STPM+AM model varies slightly throughout the entire process. After 40 iterations, it is more stable at 0.15, which is 0.15 lower than the STPM model. This shows that the performance of the STPM+AM model is more stable.

When analyzing the performance of the STPM anomaly detection model integrated with the AM, this model is compared with several other commonly used data anomaly detection models. The performance evaluation index ROC curve of the model is used to evaluate the detection effect of the model. The area under the ROC curve is AUC. Generally speaking, the larger the value of AUC, the better the performance of the model. The result is shown in Figure 7.

From Figure 7, the AUC value of STPM+AM model is 0.968. The AUC value of STPM model is 0.924, which is 0.044 lower than STPM+AM model. The AUC value of CNN model is 0.745, which is 0.223 lower than that of STPM+AM model. The AUC value of DifferNet model is 0.859, which is 0.109 lower than that of STPM+AM model. The above results can show that the AUC value of STPM+AM model performs better. Therefore, the improved STPM based on AM can effectively enhance the performance of the model in the anomaly detection.

Aiming at the performance of the defect calculation method in the suspended bridge inspection vehicle system. The transverse and longitudinal dimensions of the cracks are tested and compared with the actual dimensions.

Table 1 shows the comparison between the predicted results and the actual results. In Table 1, the edge length of the crack obtained by the findContours function algorithm is slightly larger than the actual length and width of the crack. The side length errors of No. 1 transverse crack are 0.56 mm and 0.035 mm. The side length errors of the No. 2 transverse crack are 1.57 mm and 0.009 mm. The side length errors of the No. 3 transverse crack are 0.73 mm and 0.026 mm, respectively. The side length errors of No. 1 longitudinal crack are 1.53 mm and 0.023 mm, respectively. The side length errors of No. 2 longitudinal crack are 1.37 mm and 0.023 mm, respectively. The side length errors of No. 3 longitudinal

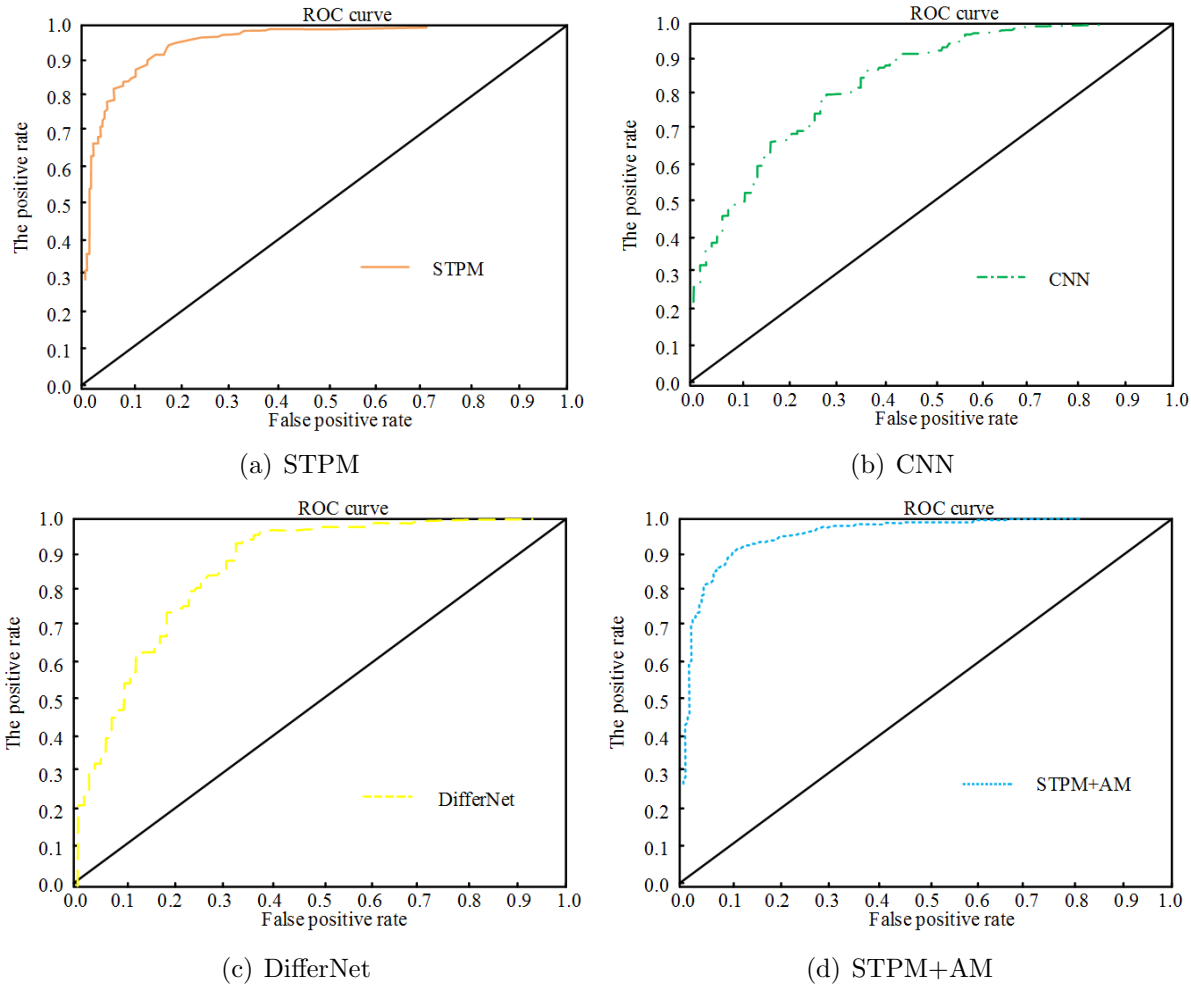

(a) STPM (b) CNN

(c) DifferNet (d) STPM+AM

FIGURE 7. ROC curves of four anomaly detection models

TABLE 1. Transverse and longitudinal dimension test of cracks

Category	Serial No.	Area (pixel)	Perimeter (mm)	Radian of arc	Pixels	Length of crack (mm)	Actual length of crack (mm)	Width of crack (mm)	Actual width of crack (mm)
Transverse crack	1	216	77.6	0.45	592	7.41	6.85	0.364	0.329
	2	550	178.2	0.22	1417	17.91	16.34	0.385	0.376
	3	146	44.1	0.34	481	6.07	5.34	0.293	0.267
Longitudinal crack	1	5936	1458	0.029	8764	109.06	107.53	0.674	0.651
	2	307	109.7	0.35	937	11.23	9.86	0.331	0.308
	3	261	90.3	0.41	652	8.34	8.07	0.385	0.364

crack are 0.27 mm and 0.021 mm, respectively. The width error of the crack is about 0.03 mm. The length error of the crack is about 1.5 mm. The crack error data detected by the algorithm is small. The errors are all distributed within a reasonable interval class, indicating that the crack calculation method proposed in the study is effective.

4.2. **Application analysis of defect detection technology based on suspended bridge inspection vehicle.** The suspended bridge inspection vehicle proposed in the study is applied to the defect inspection of the appearance of the bridge beam bottom. 3,500 images in the test set are preprocessed for abnormal detection and classification. The classification accuracy obtained is shown in Figure 8.

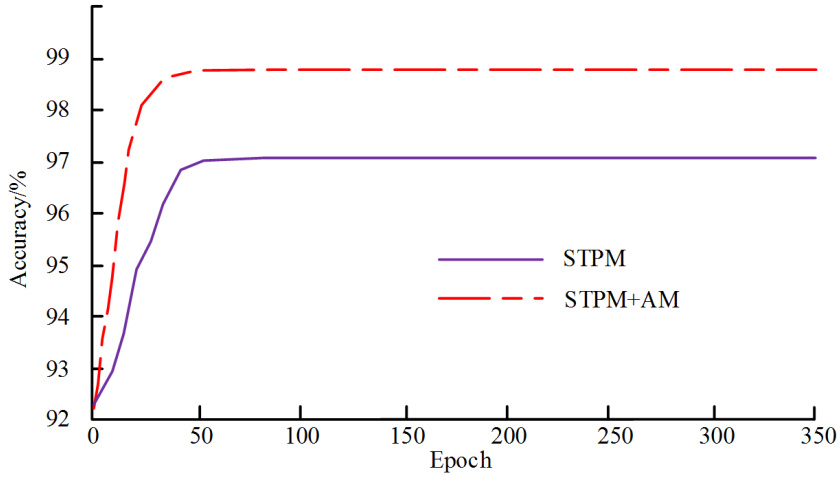

FIGURE 8. Comparison of image detection results of suspended bridge inspection vehicle

In Figure 8, the accuracy of the STPM+AM anomaly detection model is significantly higher than that of the STPM model. From the change trend of the curve, in the early stage of the iteration, the accuracy rates of the two anomaly detection models are continuously increasing. After the number of iterations reaches 50, the change trend of the two models gradually decreases. After the accuracy curve stabilized, the accuracy of the STPM model is 97.1%. The accuracy of the STPM+AM model is 98.8%, which is 1.7% higher than that of the STPM model. This shows that the STPM anomaly detection model integrated into the AM proposed by the study has a higher accuracy rate in used.

The cracks in the classified bridge defect image are quantified and calculated. The differences between the calculated results and the actual measurement results are shown in Table 2.

From Table 2, the side length of the crack measured by the algorithm is smaller than the actual length and width of the crack. The side length error rates of No. 1 crack

TABLE 2. Comparison of error results of bridge cracks

Category	Serial No.	Length measured by algorithm (mm)	Actual length of crack (mm)	Length error (%)	Width measured by algorithm (mm)	Actual width of crack (mm)	Width error (%)
Transverse crack	1	1065.34	1024.51	3.83	75.92	68.85	9.31
	2	215.56	197.43	8.41	15.97	15.14	5.20
	3	364.83	347.59	4.73	21.69	19.87	8.40
Longitudinal crack	4	2845.71	2618.93	8.00	187.54	174.38	7.02
	5	457.65	432.89	5.41	28.97	27.35	5.60
	6	78.49	77.25	1.58	7.29	7.03	3.57

are 3.83% and 9.31%, respectively. The side length error rates of No. 2 crack are 8.41% and 5.2%, respectively. The side length error rates of No. 3 crack are 4.73% and 8.4%, respectively. The side length error rates of No. 4 crack are 8% and 7.02%, respectively. The side length error rates of No. 5 crack are 5.41% and 5.6%, respectively. The side length error rates of No. 6 crack are 1.58% and 3.57%, respectively. The maximum error rate of length is 8.41%, and the average error rate is 5.33%. The maximum error rate of width is 9.31%, and the average error rate is 6.52%. The errors of the cracks detected by the algorithm are all less than 10%, and the error rate is small, which shows that the crack calculation method proposed in the study has a high accuracy. It can meet the requirements of detection accuracy and be applied to practical detection.

5. **Conclusion.** The safety of bridge structure can effectively reduce the occurrence of traffic safety accidents and ensure the safety of people's property and life. Early bridge defect detection is an effective measure to ensure bridge safety. At this stage, the practicality of bridge defect detection technology is limited. It cannot meet the cost and accuracy requirements of bridge detection. The suspended bridge inspection vehicle can effectively break through the limitation of the environment to realize the detection of bridge appearance defects. Based on this, the suspended bridge inspection vehicle is proposed to detect bridge appearance defects in a timely manner. The AM is used to improve the STPM image anomaly detection model of the inspection vehicle. At the same time, the findContours function is used to calculate the length and width of cracks. The experimental results show that the STPM+AM image anomaly detection model of the suspended bridge inspection vehicle has an accuracy of 96.5% during the training process. The loss value is 0.15. The ROC value is 0.968. The crack length and width errors calculated by the findContours function are both within a reasonable range. The average error rate of length is 5.33%. The average error rate of width is 6.52%. Therefore, the image recognition model based on the AM proposed in the study has higher accuracy and recognition efficiency, which has more ideal practical application performance. However, there are many types of bridge defects. Bridge cracks are temporarily selected for discussion in this study. Other bridge defects need to be quantitatively analyzed in follow-up research.

Acknowledgment. The study was supported by the Special Research Fund of Academicians of China Communications Group (YSZX-03-2020-01-B, YSZX-03-2021-02-B).

REFERENCES

[1] M. A. Qurishee, W. Wu, B. Atolagbe, J. Owino, I. Fomunung and M. Onyango, Creating a dataset to boost civil engineering deep learning research and application, *Engineering*, vol.12, no.3, pp.151-165, 2020.

[2] M. M. Karim, R. Qin, G. Chen and Z. Yin, A semi-supervised self-training method to develop assistive intelligence for segmenting multiclass bridge elements from inspection videos, *Structural Health Monitoring*, vol.21, no.3, pp.835-852, 2022.

[3] Z. Xu, Z. Du, Z. Yang and J. Zhou, Research on vehicle-bridge vertical coupling dynamics of monorail based on multiple road excitations, *Mechanika*, vol.26, no.4, pp.301-310, 2020.

[4] E. Jeong, J. Seo and J. Wacker, Grayscale drone inspection image enhancement framework for advanced bridge defect measurement, *Transportation Research Record*, vol.2675, no.8, pp.603-612, 2021.

[5] J. Ye, G. Xia, F. Liu and Q. C. Qiang, Weld defect inspection based on machine vision and weak magnetic technology, *Insight: Non-Destructive Testing and Condition Monitoring*, vol.63, no.9, pp.547-553, 2021.

[6] F. Ogawa and Y. Chikata, Analysis on the utilization of opinion of bridge inspection results using topic model for maintenance and management, *Materials Transactions*, vol.61, no.12, pp.2428-2434, 2020.

[7] Y. Z. Ayele, M. Aliyari, D. Griffiths and E. L. Droguett, Automatic crack segmentation for UAV-assisted bridge inspection, *Energies*, vol.13, no.23, pp.1-16, 2020.
[8] T. Ikeda, S. Minamiyama, S. Yasui, K. Ohara and T. Fukuda, Stable camera position control of unmanned aerial vehicle with three-degree-of-freedom manipulator for visual test of bridge inspection, *Journal of Field Robotics*, vol.36, no.7, pp.1212-1221, 2019.
[9] W. Minkina, Problems of remote temperature measurement of small objects of electricity power systems – On the example of lashing clamps of bridge connections on high voltage poles, *Energies*, vol.14, no.16, pp.1-11, 2021.
[10] H. Li, B. F. Spencer, M. R. Saleem, J. W. Park, J. H. Lee, H. J. Jung and M. Z. Sarwar, Instant bridge visual inspection using an unmanned aerial vehicle by image capturing and geo-tagging system and deep convolutional neural network, *Structural Health Monitoring*, vol.20, no.4, pp.1760-1777, 2020.
[11] J. Won, J. W. Park, C. Shim and M. W. Park, Bridge-surface panoramic-image generation for automated bridge-inspection using deepmatching, *Structural Health Monitoring*, vol.20, no.4, pp.1689-1703, 2020.
[12] H. Zhao, Y. Ding, A. Li, Z. Ren and K. Yang, Live-load strain evaluation of the prestressed concrete box-girder bridge using deep learning and clustering, *Structural Health Monitoring*, vol.19, no.4, pp.1051-1063, 2019.
[13] M. Yuan and Q. Dai, A novel deep pixel restoration video prediction algorithm integrating attention mechanism, *Applied Intelligence*, vol.52, no.5, pp.5015-5033, 2022.
[14] J. Cheng, S. Peng, R. Cheng, X. Wu and X. Fang, Burst area identification of water supply network by improved DenseNet algorithm with attention mechanism, *Water Resources Management*, vol.36, no.14, pp.5425-5442, 2022.
[15] M. Huang, S. Liu, Z. Li, S. Feng and F. Shu, Remote sensing image fusion algorithm based on two-stream fusion network and residual channel attention mechanism, *Wireless Communications and Mobile Computing*, no.6, pp.1-14, 2022.
[16] J. Shao and H. Ge, Siamese object tracking algorithm combining residual connection and channel attention mechanism, *Journal of Computer-Aided Design & Computer Graphics*, vol.33, no.2, pp.260-269, 2021.
[17] Y. Liu, Q. Wang, H. Zhang, Y. Liu and K. Zhao, Real-time defect detection of metal surface based on improved YOLOv4, *International Journal of Innovative Computing, Information and Control*, vol.18, no.4, pp.1329-1338, 2022.
[18] Y. Li, X. Yu and Q. Bao, Image inpainting algorithm based on neural network and attention mechanism, *Journal of Intelligent and Fuzzy Systems*, vol.38, no.10, pp.1-12, 2019.
[19] H. Wu and G. Liu, Split-merge-excitation: A robust channel-wise feature attention mechanism applied to MDNet tracking, *Multimedia Tools and Applications*, vol.81, no.28, pp.40737-40754, 2022.
[20] J. Baek, Y. Kim, B. Chung and C. Yim, Linear spectral clustering with contrast-limited adaptive histogram equalization for superpixel segmentation, *IEIE Transactions on Smart Processing and Computing*, vol.8, no.4, pp.255-264, 2019.
[21] M. Sahani, B. K. Swain and P. K. Dash, FPGA-based favourite skin colour restoration using improved histogram equalization with variable enhancement degree and ensemble extreme learning machine, *IET Image Processing*, vol.15, no.6, pp.1247-1259, 2021.
[22] W. T. Ma, J. H. Qin, X. Y. Xiang, Y. Tan, Y. J. Luo and N. N. Xiong, Adaptive median filtering algorithm based on divide and conquer and its application in CAPTCHA recognition, *Computers, Materials and Continua*, vol.58, no.3, pp.665-677, 2019.
[23] A. Chefrour and L. Souici-Meslati, AMF-IDBSCAN: Incremental density based clustering algorithm using adaptive median filtering technique, *Informatica*, vol.43, no.4, pp.495-506, 2019.
[24] C. Li, M. Qi, M. Dong, S. H. Fan, Z. W. Liu and X. M. Zhao, End-to-end autonomous driving decision model joined by attention mechanism and spatiotemporal features, *IET Intelligent Transport Systems*, vol.15, no.9, pp.1119-1130, 2021.
[25] T. Song, Y. Li, F. Meng, P. F. Xie and D. Y. Xu, A novel deep learning model by BiGRU with attention mechanism for tropical cyclone track prediction in the northwest Pacific, *Journal of Applied Meteorology and Climatology*, vol.61, no.1, pp.3-12, 2022.
[26] C. Andry, S. Rhio, Meiliana and T. Sansiri, Answer generation with an attention mechanism dual encoder LSTM, *ICIC Express Letters*, vol.15, no.7, pp.701-709, 2021.

Author Biography

Jun Xu received the B.Sc. degree in Civil Engineering (Bridge and Tunnel) from Tongji University, China, 1994; the M.Sc. degree in Bridge and Tunnel Engineering from Tongji University, China, 1997. Now, he is studying for a doctor's degree in the College of Civil Engineering of Tongji University.

Mr. Xu, senior engineer, serves as the deputy chief engineer of CCCC Highway Consultants Co., Ltd. His research direction is the structural design of bridges. He has published over 15 papers in journals and conferences. He is participating in some research projects funded from National Natural Science Foundation of China.

Qingrong Jia received the B.Sc. degree in Civil Engineering (Road, Bridge, and River-Crossing Engineering) from Chang'an University, China, 2008; the M.Sc. degree in Traffic and Transportation Engineering from Chang'an University, China, 2019.

Mr. Jia, senior engineer, serves as the deputy chief engineer of Guangdong Bay Area Transportation Construction Investment Co., Ltd. His research direction is the expressway design and construction management. He has published over 3 papers in journals and conferences.

Tingqi Qiu received the B.Sc. degree in Mechanical Engineering and Automation from Southwest Jiaotong University, China, 2004.

Mr. Qiu serves as the chief engineer of Chengdu Xinzhu Road & Bridge Machinery Co., Ltd. His research interests include bridge bearings, expansion joints, seismic isolation and bridge inspection robots. He has published over 10 papers in journals and conferences. He has obtained more than 10 Chinese invention patents.

Yuanqing Xu received the B.Sc. degree in Civil Engineering (Road and Bridge) from Jilin University, China, 2009; the M.Sc. degree in Bridge and Tunnel Engineering from Beijing Jiaotong University, China, 2012. Now, he is studying for a doctor's degree in the College of Civil Engineering of Hunan University.

Mr. Xu serves as the laboratory director of CCCC Highway Bridges National Engineering Research Centre Co., Ltd. His research direction is the structural system and seismic isolation technology of long-span bridges. He has published over 20 papers in journals and conferences. He is participating in some research projects funded from National Natural Science Foundation of China.

Minglong Wu received the B.Sc. degree in Mechanical Design Manufacturing and Automation from Hunan University of Technology, China, 2015.

Mr. Wu serves as an R&D engineer of Chengdu Xinzhu Road & Bridge Machinery Co., Ltd. His research interests include bridge inspection robots, bridge bearings, and expansion joints. He has published 7 papers in journals and conferences.

Bing Yang received the B.Sc. degree in Electrical Engineering and Automation from Xihua University, China, 2007.

Mr. Yang serves as an electrical R&D engineer of Chengdu Xinzhu Road & Bridge Machinery Co., Ltd. His research interests include electrical automatic control of bridge inspection vehicles, inspection vehicle IoT platform, and CNC machine tools. He has obtained 2 Chinese invention patents.